Journal of Structural Biology 166 (2009) 107–111

Contents lists available at ScienceDirect

Journal of Structural Biology

journal homepage: www.elsevier.com/locate/yjsbi

Crystallization Note

AcrB et al.: Obstinate contaminants in a picogram scale. One more bottleneck in the membrane protein structure pipeline

Georgios Psakis [a,b], Julia Polaczek [a], Lars-Oliver Essen [a,*]

[a] Department of Chemistry, Philipps-University Marburg, Hans-Meerwein-Strasse, 35033 Marburg, Germany
[b] Department of Plant Physiology, Justus-Liebig University Giessen, Schenkenbergstrasse 3, D-35390 Giessen, Germany

ARTICLE INFO

Article history:
Received 15 November 2008
Received in revised form 17 December 2008
Accepted 18 December 2008
Available online 30 December 2008

Keywords:
AcrB
Succinate dehydrogenase
Heterologous expression
Picogram crystallization
Membrane protein contaminants
Structural genomics

ABSTRACT

Heterologous expression of integral membrane proteins from *Helicobacter pylori* 26695 in *Escherichia coli* enabled the identification of 17 candidates for purification and subsequent crystallization. 45% of the purified proteins were contaminated with what was later identified as the multidrug efflux pump (AcrB) of *E. coli*, and 17% with the succinate dehydrogenase. While additional purification steps ensured removal of succinate dehydrogenase, they failed to remove AcrB completely, leaving picogram amounts present in fractions intended for 3D-crystallization. Two of these targets, the Na^+ dependent D-glucose/D-galactose transporter (GluP-HP1174) and the carbon starvation protein A (CstA-HP1168), produced small crystals (<40 μm). Crystals from the GluP preparation diffracted to 4.2 Å resolution and belonged to the rhombohedral space group *H*32. Subsequent molecular replacement proved that these crystals were derived from a contaminant, the efflux transporter AcrB. This unexpected crystallization of AcrB from picogram amounts was observed in six new conditions. The systematic occurrence of AcrB in membrane preparations stems from the upregulation of its transcription in response to the stress induced by the expression of a selected target. This, along with its tendency to crystallize in the picogram scale, poses a serious concern in membrane protein expression using heterologous hosts harbouring AcrB.

In recent years membrane protein structural genomics has focused on increasing the number of targets going through the pipeline from gene to structure in a rapid and cost-efficient way. Often, however, many of the standard quality controls are bypassed in order to ensure the fast screening of the highest number of targets possible. In previous work (Psakis et al., 2007), we proposed that a medium-throughput genomics approach can be more effective, as it allows for the fine-tuning and control of parameters that can interfere with the efficiency of expression and solubilization of a selected target and with the quality of its purification. The latter approach was used for the identification of suitable *Helicobacter pylori* 26695 integral membrane proteins for structural studies (Psakis et al., 2007). The Na^+/H^+ D-glucose/D-galactose symporter (GluP-HP1174) and the carbon starvation protein A (CstA-HP1168) were two of those proteins.

GluP is the only porter responsible for Na^+-driven D-glucose/D-galactose transport in *H. pylori* (Mendz et al., 1995; Tomb et al., 1997). Since no mammalian hexose-transporters show significant alignments with GluP of *H. pylori*, and glucose transport into *H. pylori* is not susceptible to inhibitors that affect mammalian transporters (Mendz et al., 1995), this protein represents an ideal target for structure-based drug design. CstA, on the other hand, belongs to a family of putative integral membrane transporters predicted to be responsible for the entry of amino acid and/or carboxylic-based substrates into the bacterium (Tomb et al. 1997). The latter substrates provide the main and preferred carbon energy source in *H. pylori*. Despite extensive research on the carbon-starvation metabolism of bacterial hosts, however, little is known about the structure-function relationship of these transporters making them thus to attractive targets for future research.

Here, we report the co-purification of selected targets with the multi-drug efflux pump (AcrB) and/or succinate dehydrogenase. Both contaminating proteins display similar features: (1) the levels of their gene transcription can be induced under standard experimental conditions, (2) they show affinity to Ni^{2+} immobilised matrices, and (3) they crystallize in the same space group. Although additional purification steps can result in the complete removal of succinate dehydrogenase, only partial removal of AcrB is possible and the presence of even picogram amounts of the latter is enough to drive formation of its rhombohedral crystal form.

GluP$(His)_6$ was purified at 4 °C by high-flow Ni^{2+}–NTA affinity chromatography (Qiagen) compatible with the Äkta Prime purifier (Amersham Biosciences). The protein was extracted from the inner membranes of BL21(DE3) *Escherichia coli* cells in 50 mM Tris–HCl (pH 8.5), 300 mM NaCl, 0.2 mM $MgCl_2$, 10% glycerol, 20 mM β-mercaptoethanol, 10 mM imidazole and 0.1% dodecyl-β-D-

* Corresponding author. Fax: +49 6421 2822012.
E-mail addresses: essen@chemie.uni-marburg.de, georgios.psakis@bot3.bio.uni-giessen.de (L.-O. Essen).

1047-8477/$ - see front matter © 2009 Elsevier Inc. All rights reserved.
doi:10.1016/j.jsb.2008.12.007

maltopyranoside (DDM-Applichem)—buffer A- by gentle mixing at 4 °C for 16 h. Following centrifugation at 109,000*g* for 1 h at 4 °C, the supernatant containing the solubilized fractions was filter-sterilized (0.22 μm filter-Millipore) and was loaded to a Ni^{2+}–NTA column previously equilibrated with 10 column volumes of buffer A. The bound protein was further washed with 60–80 column volumes of buffer A, and eluted with a step gradient created by mixing buffers A and B (buffer A with 500 mM imidazole). Fractions containing the tagged protein were collected and desalted in a PD-10 column (Amersham Biosciences). The protein was eluted in 25 mM sodium-citrate buffer (pH 5.0), 5% glycerol, 20 mM β-mercaptoethanol and 0.05% DDM and concentrated to 6–8 mg ml^{-1} by using a centricon Amicon with a 50 kDa cutoff (Millipore). For the final polishing step, the purified protein was subjected to ion-exchange chromatography (Sartorius) to ensure the removal of excess detergent and other protein contaminants. CstA$(His)_6$ was solubilized in 2% decyl-β-D-maltoside (DM; Applichem), and was concentrated to 4–6 mg ml^{-1} in a buffer containing 50 mM Hepes (pH 7.5), 5% glycerol, 2 mM β-mercaptoethanol, and 0.2% DM.

The purification efficiency for both proteins was assessed by 15% SDS–PAGE electrophoresis (Fig. 1). The identity of both the desired and contaminating proteins was confirmed by Western blotting and MALDI-TOF analysis of their trypsin-generated products.

Crystallization screenings were carried out with a Cartesian Mycrosys 4004 robot (Genomic Solutions), using the sitting drop method in a 96-well plate set-up. Protein solution (4–8 mg ml^{-1}) was mixed in a 1:1 ratio with mother liquor (0.05 μl protein plus 0.05 μl liquor). More than 864 conditions from screens from Qiagen and Sigma were tested per batch of purified protein. Samples were incubated at 289 K. In the case of GluP$(His)_6$ preparation, crystals appeared after 4 months and kept growing for further 2 months (Fig. 2). Crystals were reproducible with different protein batches, and optimisation of the original conditions (lowering the PEG content by 2%; Pos and Diederichs, 2002) resulted in mature crystals (30–50 μm) within two weeks. In the case of the CstA$(His)_6$ preparation, crystals appeared after 2 weeks and reached a maximum size of 40 μm. Successful crystallisation conditions are listed in Table 1. Several pyramidally shaped crystals were screened at beam-lines ID23 (ESRF, Grenoble) and PX06SA (SLS, Villigen) and found to diffract to 3.8–4.6 Å resolution. One complete dataset was recorded from a single putative GluP crystal at beam-line PX06SA at the SLS, Villigen (Table 2). After indexing (Powell, 1999) scaling (Bolotovsky et al. 1998) and taking radiation damage, during data collection, into account (300 images; 0.5° oscillation, 1 s exposure) the crystals were assigned to the rhombohedral space group *R*32 (hexagonal setting *H*32, $a = b = 146.5$ Å, $c = 515$ Å) and diffracted up to at least 4.2 Å resolution (Fig. 2B). Overall, the crystals comprise three or four monomers (MW 43951 Da) per asymmetric unit with a predicted solvent content of 69% or 59%, respectively.

Initial attempts to solve the GluP$(His)_6$ structure by molecular replacement (*MOLREP*—Vagin and Teplyakov, 1997; ccp4i—Leslie, 1992; Potterton et al., 2003) using the *E. coli* lactose permease (1PV6) or the *E. coli* glycerol-3-phosphate transporter (1PW4) models failed. This was not surprising given the low sequence identity (⩽12%) to the corresponding proteins and the limited data quality. At this stage, however, and in order to exclude the possibility of the crystallization of a contaminating protein, we searched for membrane proteins crystallizing in the *R*32 space group or its hexagonal setting *H*32. The *E. coli* acriflavine resistance protein B (AcrB, PDB code 1IWG, $a = b = 144.5$ Å, $c = 519.2$ Å) and *E. coli* respiratory complex II (succinate dehydrogenase, PDB code 1NEK, $a = b = 138.8$ Å, $c = 521.9$ Å) were two of the proteins we identified. Parallel to this approach we isolated three barely visible bands of the SDS–PAGE gel (Fig. 1A) and subjected their trypsin-generated fragments to MALDI-TOF mass-spectrometric analysis. The top band was identified as AcrB (Suppl. S1), whilst the other two failed to produce a signal. Molecular replacement by PHASER using the AcrB structure as model accordingly produced an unambiguous solution (*Z*-scores for rotation/translation function: 10.3/39.4), confirming the scenario that the crystals were not of GluP$(His)_6$ but of AcrB. The abundance of AcrB in the fractions was <0.1% as judged by densitometry of scanned SDS–PAGE lanes. The total amount of AcrB present in the crystallization drop was hence in the range of 100–500 pg, providing as yet the first example of a membrane protein crystallizing from picogram amounts. Additionally, six new crystallization conditions for AcrB were identified (Table 1). Crystallization of AcrB, so far, only occurred in our screens in the presence of maltosides and/or glucosides.

AcrB poses a serious problem, when heterologous proteins are expressed in *E. coli* or other hosts harbouring multi-drug resistance proteins, because its expression is induced by stress. Consequently,

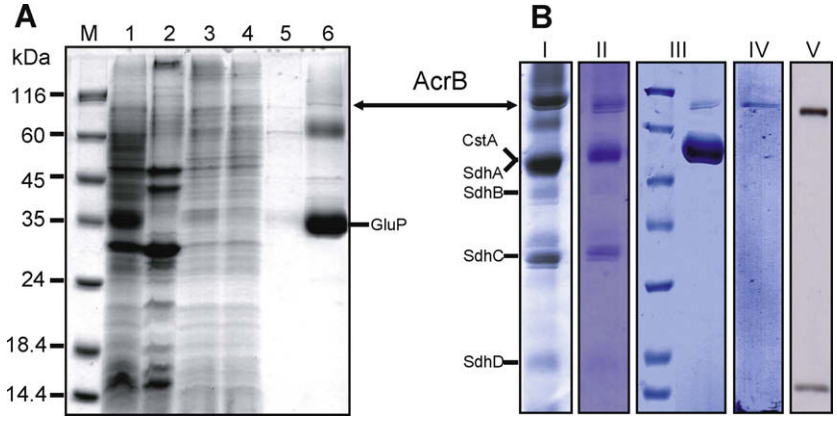

Fig. 1. Purification profiles of GluP$(His)_6$ (A) and CstA$(His)_6$ (B) on 12% Coomassie Blue stained SDS–PAGE gels. (A) Lane M, molecular weight markers (Fermentas, 2 μg); Lane 1, *E. coli* BL21(DE3) membranes containing GluP$(His)_6$ (30 μg); Lane 2, insoluble material after detergent extraction (30 μg); Lane 3, detergent extract of *E. coli* BL21(DE3)/GluP$(His)_6$ (30 μg); Lane 4, Ni^{2+}–NTA chromatography (10 mM imidazole) flowthrough fraction (30 μg); Lane 5, Ni^{2+}–NTA chromatography (40 mM imidazole) washing fraction (30 μg); Lane 6, purified and concentrated GluP$(His)_6$ (30 μg). (B) I, Ni^{2+}–NTA co-purification of CstA$(His)_6$, succinate dehydrogenase complex (subunits SdhA, B, C, and D indicated) and AcrB (30 μg); II, purified complex, contaminated with AcrB after cation-exchange of the previous fractions (20 μg); III, purified and concentrated CstA contaminated with AcrB (30 μg); IV, purified native *E. coli* AcrB (0.05 μg) shown as control; V, detection of native *E. coli* AcrB (0.05 μg) by anti-His_5 antibody (bottom band-dye front).